ADVANCED MATERIALS
www.advmat.de

Dynamic Hyaluronan Hydrogels with Temporally Modulated High Injectability and Stability Using a Biocompatible Catalyst

*Junzhe Lou, Fang Liu, Christopher D. Lindsay, Ovijit Chaudhuri, Sarah C. Heilshorn, and Yan Xia**

Injectable and biocompatible hydrogels have become increasingly important for cell transplantation to provide mechanical protection of cells during injection and a stable scaffold for cell adhesion post-injection. Injectable hydrogels need to be easily pushed through a syringe needle and quickly recover to a gel state, thus generally requiring noncovalent or dynamic cross-linking. However, a dilemma exists in the design of dynamic hydrogels: hydrogels with fast exchange of cross-links are easier to eject using less force, but lack long-term stability; in contrast, slow exchange of cross-links improves stability, but compromises injectability and thus the ability to protect cells under flow. A new concept to resolve this dilemma using a biocompatible catalyst to modulate the dynamic properties of hydrogels at different time points of application to have both high injectability and high stability is presented. Hyaluronic acid based hydrogels are formed through dynamic covalent hydrazone cross-linking in the presence of a biocompatible benzimidazole-based catalyst. The catalyst accelerates the formation and exchange of hydrazone bonds, enhancing injectability, but rapidly diffuses away from the hydrogel after injection to retard the exchange and improve the long-term stability for cell culture.

Injectable hydrogels that encapsulate bioactive therapeutics and cells can be administered via simple and minimally invasive procedures.[1] These hydrogels not only deliver cells at the target site through a needle but also provide a 3D scaffold post-injection to support cell viability and function. The majority of injectable hydrogels are shear-thinning and self-healing, which exhibit viscous flow under an applied shear stress and time-dependent recovery upon removing the stress.[2] These hydrogels can be prepared ex vivo with cells and therapeutics encapsulated, and then flow through a needle under force and recover its modulus at the target site. Such injectable properties require the hydrogels to be noncovalently or dynamically cross-linked. Many interactions have been explored to prepare dynamic hydrogels, including peptide self-assembly, electrostatic attraction, hydrogen bonding, supramolecular complexation, protein interactions, and dynamic chemical bonds.[3] But few of such systems have been demonstrated for cell delivery via injection.[4] Injectable hydrogels based on association of protein polymers have been reported to protect cells under shear stress, which is attributed to a shear-banding mechanism to prevent the damage of cell membranes.[5] The shear banding and plug-flow profiles localize the shear deformation within narrow regions close to the needle wall, therefore shielding most cells from extensional and shear flow.[6] Relatively weak physical interactions and dynamic bonds with fast exchange kinetics facilitate injection, but often lead to rapid erosion of the gel. The lack of long-term stability post-injection limits the biological applications of these materials to provide cell scaffolding or prolonged drug release. Recently, dual cross-linked hydrogels have been developed to enable an additional cross-linking step post-injection:[4d,7] The first network is weakly cross-linked ex vivo via noncovalent interactions, and the second cross-linking is implemented in situ using UV irradiation,[7a–c] temperature,[4d,7d,e] or pH variation[7f,g] to improve the mechanical properties and stability of the hydrogels. The dual cross-linking design is effective at increasing material stability, but the secondary cross-linking step may require nonphysiological conditions and necessarily vary the network structures and mechanical properties of hydrogels, which can be incompatible with biomedical applications.

It would be ideal if the exchange dynamics of cross-linking of injectable hydrogels could be simply modulated at different time points under physiological conditions without altering the equilibrium network structure, chemical composition, or scaffold stiffness. That is, rapid cross-link exchange during injection to minimize cell damage, but slow cross-link exchange

J. Lou, Dr. F. Liu, Prof. Y. Xia
Department of Chemistry
Stanford University
Stanford, CA 94305, USA
E-mail: yanx@stanford.edu
J. Lou, C. D. Lindsay, Prof. S. C. Heilshorn
Department of Materials Science and Engineering
Stanford University
Stanford, CA 94305, USA
Prof. O. Chaudhuri
Department of Mechanical Engineering
Stanford University
Stanford, CA 94305, USA
The ORCID identification number(s) for the author(s) of this article can be found under https://doi.org/10.1002/adma.201705215.

DOI: 10.1002/adma.201705215

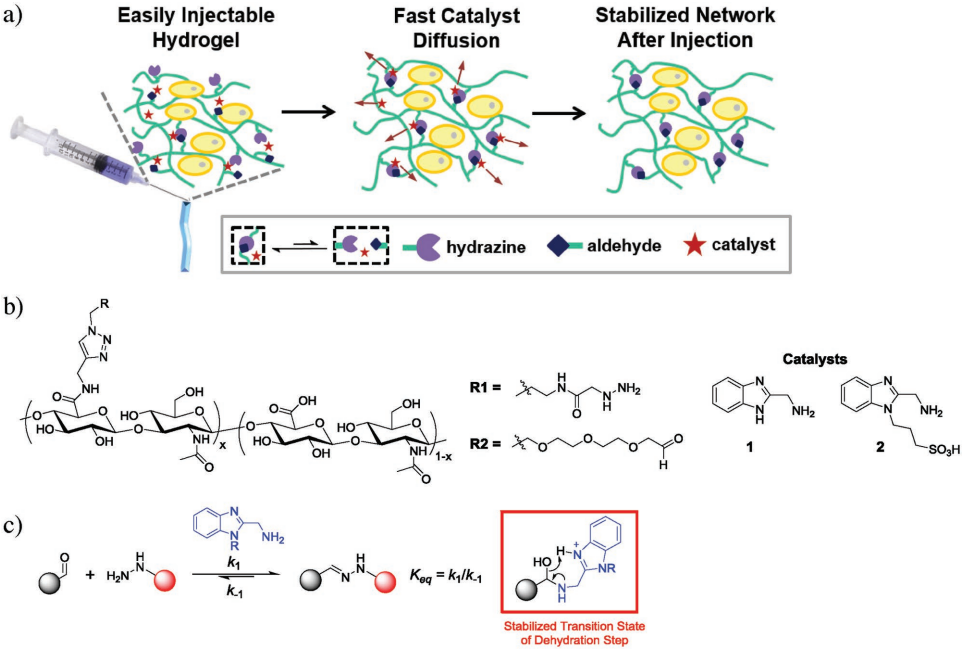

Figure 1. a) Schematic representation of using diffusible organocatalyst to temporally modulate dynamic properties of hydrazone cross-linking hydrogels. During injection, the incorporated catalyst promotes rapid exchange of hydrazone cross-links and rearrangement of network to facilitate flow. After injection, the catalyst rapidly diffuses away to slow down hydrazone exchange, resulting in the identical network structure with improved stability. b) Chemical structures of hydrazine and aldehyde-modified HA polymers (left) and catalysts used to accelerate hydrazone exchange (right). c) Scheme of catalyst-accelerated hydrazone equilibrium, where the catalyst forms a seven-membered transition state with aldehyde to lower the energy barrier of the rate-determining dehydration step.[10b]

post-injection to enhance long-term network stability. We report a novel approach to achieve this goal by temporally modulating the exchange dynamics of hydrazone cross-linking using an incorporated biocompatible organocatalyst under physiological conditions, without changing the network structure or scaffold modulus. The catalyst accelerates both the formation and exchange of hydrazone bonds to facilitate gel shear-thinning and injectability, but quickly diffuses out of the hydrogel after injection, leading to much slower bond exchange to stabilize the matrix (**Figure 1**a). Since a catalyst only accelerates the rate of bond exchange but does not affect the thermodynamic equilibrium, the network structure remains unchanged.

Hydrazone formation is a widely used bioconjugation chemistry, and the rates of formation and dissociation of hydrazone bonds are dependent on the structures of aldehyde and hydrazine.[8] The dynamic nature of the hydrazone bond makes it well suited for the preparation of viscoelastic hydrogels.[9] Kool and co-workers have recently studied a variety of compounds as potential organocatalysts to accelerate hydrazone formation and pointed out the importance of general acid/base catalysis in accelerating the rate-limiting dehydration step.[10] We reasoned that these catalysts should also accelerate the reverse reaction and thus the exchange of hydrazone bonds, thereby enhancing the ability of hydrazone cross-linking hydrogels to flow through a syringe. We chose HA as the polymer backbone to form these hydrogels, since it is a biocompatible, naturally abundant polysaccharide in human tissue and plays an important role in many biological processes.[11] HA is a relatively sensitive natural polymer that degrades under acidic, basic, and oxidative conditions. Therefore, we developed a mild strategy to modify HA with hydrazine and aldehyde groups without backbone degradation (Figure S1, Supporting Information): a predetermined amount of alkyne functionalities were attached to HA via carbodiimide coupling, which were then functionalized with hydrazine and aldehyde groups via copper catalyzed "click" reaction (Figure 1b).[12]

HA-hydrazone hydrogels can be formed easily by mixing dilute solutions of hydrazine-modified HA and aldehyde-modified HA in phosphate buffered saline (PBS, pH 7.4) at 37 °C. We chose HA with 60 kDa molecular weight and modified 12% of its carboxylate groups with aldehyde or hydrazine (Figure 1b) to study the effect of incorporated catalyst on the properties of formed hydrogels and their efficacy for cytoprotection during injection.

2-(Aminomethyl)benzimidazole **1** was reported by Kool and co-workers as one of the most efficient catalysts to accelerate hydrazone formation owing to facilitated intramolecular proton transfer in the transition state, lowering the transition state energy in the dehydration step via formation of a seven-membered ring between the catalyst and the substrate.[10b] The rates for hydrazone formation (k_1) and cleavage (k_{-1}) in the presence of **1** were measured using model reactions between hydrazine and aldehyde and modeled for a reversible second-order reaction (Figure S3, Supporting Information),[8a] and the equilibrium constant (K_{eq}) was calculated from these rate constants. **1** exhibited high catalytic activity and first-order dependence on the reaction rate (**Figure 2**a). Both k_1 and k_{-1} showed 24, 47, and 94-fold enhancement in the presence of 25, 50, and 100 × 10^{-3} M **1**, respectively (Table S1, Supporting Information), and K_{eq} remained constant and independent of the

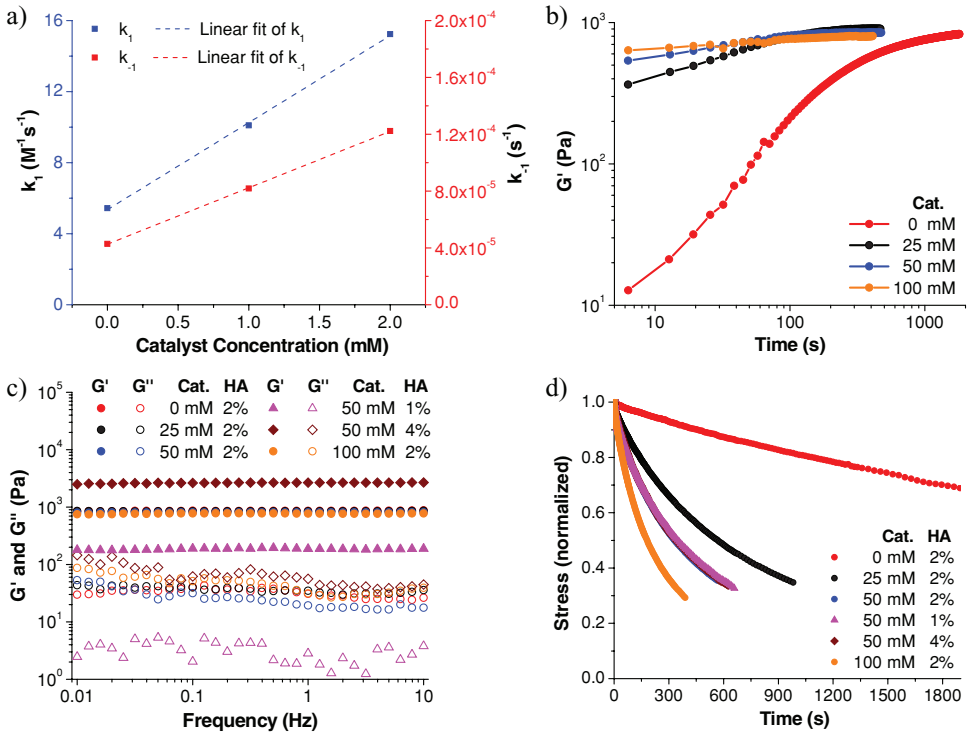

Figure 2. Effects of catalyst **1** on the hydrazone exchange reaction and properties of hydrazone cross-linked HA hydrogels. a) Measured first-order dependence of the rates of hydrazone formation (k_1) and cleavage (k_{-1}) on catalyst concentration. b) Oscillatory time sweep (2 wt% gel) showing the rate of gelation accelerated with increasing the catalyst concentration but the equilibrium modulus of the hydrogels remained the same. c) Oscillatory frequency sweep showing hydrogel modulus independent of the incorporated catalyst concentration but dependent on the HA concentration. d) Stress relaxation accelerated with increasing the catalyst concentration but independent of the HA concentration.

catalyst concentration as expected. The gelation time of our HA-hydrazone hydrogels was dramatically shortened in the presence of **1**. For a 2 wt% HA hydrogel, 30 min was required to reach equilibrium gelation without **1** (Figure 2b). In the presence of 25×10^{-3} M **1**, gelation occurred in less than 60 s and reached a final plateau shear modulus of 800 Pa in 5 min (Figure 2b). Increasing the catalyst loading to 100×10^{-3} M further shortened the time to reach equilibrium to 3 min (Figure 2b). As shown in the frequency sweep experiment (Figure 2c), stable gels were formed with a plateau storage modulus (G') around 1 kPa, which is more than an order of magnitude higher than the loss modulus (G''). The hydrogel plateau modulus remained the same regardless of the catalyst loading (examples shown using 2% HA gels at 0, 25, 50, and 100×10^{-3} M catalyst loadings in Figure 2c), confirming that the catalyst did not affect the equilibrium network structure or hydrogel modulus. In contrast, altering the HA polymer composition from 1 to 4 wt% increased the plateau modulus from 200 to 3000 Pa (Figure 2c). The dynamic exchange of hydrazone cross-links allowed the HA hydrogels to exhibit stress-relaxation behavior (Figure 2d, and Table S2, Supporting Information), which correlates to the ease of flowing under applied force. The rate of stress relaxation under constant strain was quantified by the time for the initially measured stress to relax to half of its original value, $\tau_{1/2}$. The catalyst remarkably enhanced the rate of stress relaxation for these hydrogels, decreasing $\tau_{1/2}$ from 75 min without **1** to 10 and 3 min with 25 and 100×10^{-3} M **1**, respectively (Figure 2d). Accelerated hydrazone exchange by an incorporated catalyst also allowed these hydrogels to be easily remolded macroscopically (Figure S4, Supporting Information), facilitating their injection and reprocessing. Furthermore, altering the hydrogel stiffness by tuning the HA concentration did not impact the stress-relaxation rate, as shown by the same stress-relaxation profiles between 1, 2, and 4% HA hydrogels in Figure 2d. Therefore, our design offers a unique strategy to tune the modulus and rate of stress relaxation, two important mechanical properties for dynamic hydrogel materials, *independently* and *continuously* by polymer concentration and catalyst concentration, respectively.

High cytocompatibility is needed for catalysts used in this design for biomedical applications. Concerned with the potential toxicity from the cationic nature of catalyst **1**, we synthesized a simple sulfonated derivative of **1**, thus converting it to a zwitterionic form, **2**, that we hypothesized would be more biocompatible.[13] Cytocompatibility of both **1** and **2** were evaluated using 2D cultures of human umbilical vein endothelial cells (HUVECs). HUVECs were chosen as an exemplary test cell line because they are a clinically relevant human cell type that has been broadly explored for tissue engineering and regenerative medicine applications. Significant cell death was observed in the presence of 25×10^{-3} M of **1** within several hours (**Figure 3**a). In sharp contrast, **2** exhibited high cytocompatibility, with 85% cells remaining viable after 24 h exposure at 25×10^{-3} M and negligible cell death at 5×10^{-3} M even after 3 d (Figure 3a and Figure S5, Supporting Information). Such dramatically improved cytocompatibility of **2** was attributed to its zwitterionic nature.[13] Gratifyingly, **2** was found to exhibit similar catalytic

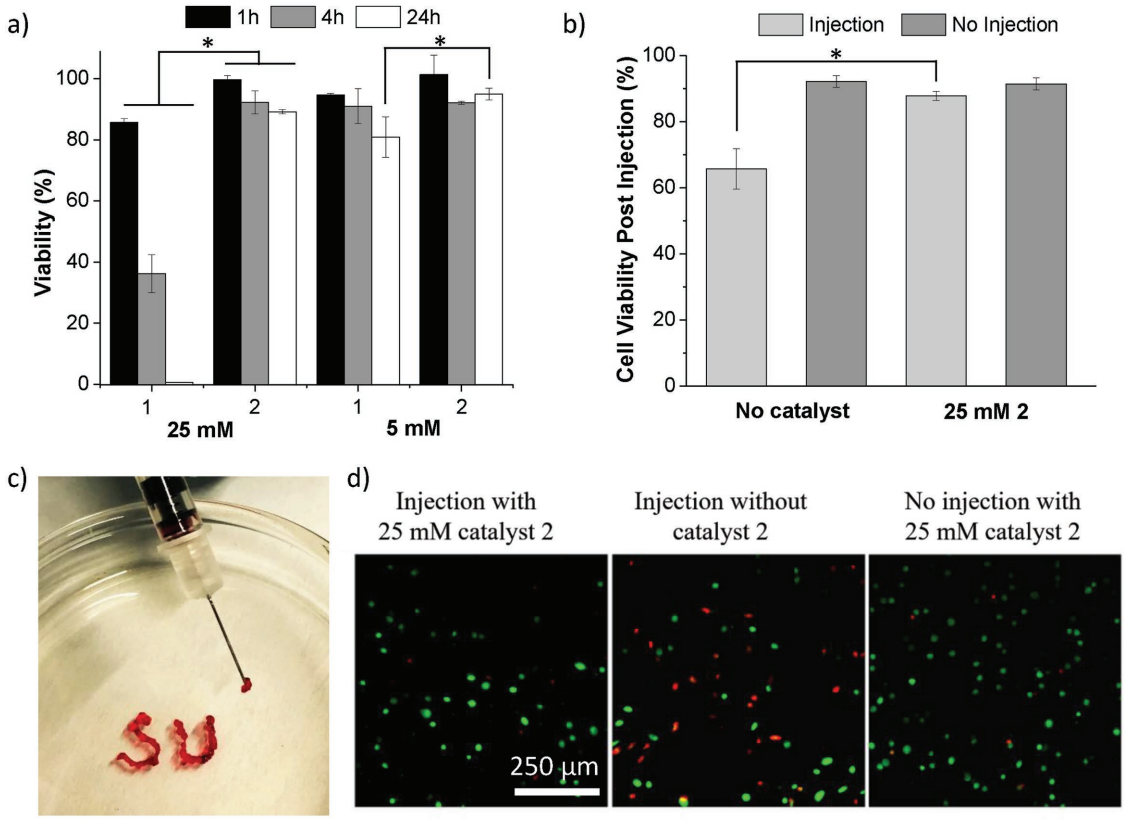

Figure 3. a) HUVEC viability after 1 h (black bars), 4 h (gray bars), and 24 h (white bars) in culture medium containing 25 and 5×10^{-3} M catalysts **1** and **2** (*$p < 0.05$, $n \geq 3$). b) Cell viability without or with 25×10^{-3} M catalyst **2** following in vitro injection of 2% hydrogel into a Petri dish through a 28 G syringe needle at 0.05 mL min^{-1} (*$p < 0.05$, $n \geq 3$). c) Photo of ejecting gels through a 28 G needle without clogging (Phenol red was added to color the hydrogel for visualization only). d) Images of LIVE/DEAD analysis for gel-encapsulated HUVECs showing viability after injection in the presence and absence of catalyst **2** and with no injection in the presence of catalyst **2**.

efficiency to **1**, and gave almost identically accelerated gelation time and tunable stress-relaxation rates as **1** at the same catalyst concentration (Figure S6, Supporting Information).

We then investigated the effect of catalyst **2** incorporated in HA-hydrazone hydrogels on the protection of encapsulated cells during injection. HUVECs were homogeneously encapsulated in 2% hydrogels containing 25×10^{-3} M **2** by rapidly mixing the cells suspended in HA solutions with catalyst and transferring to a syringe (Figure S8, Supporting Information). Hydrogel was rapidly formed in the syringe and ejected through a 28 G syringe needle. A syringe pump was used for all cell injection experiments to ensure consistent flow rate for accurate comparison between all samples. In the presence of 25×10^{-3} M **2**, the hydrogels can be ejected easily through the thin needle without clogging (Figure 3c, and Video S1, Supporting Information) and the modulus of hydrogels remained identical after injection (Figure S10, Supporting Information). In contrast, in the absence of a catalyst, the same hydrogel experienced high resistance to flow.

After injection, cells encapsulated in the hydrogels were incubated for 20 min, and cell viability was then analyzed using a standard LIVE/DEAD staining assay. In the control gel without catalyst **2**, the injection led to significant cell death with only 65% viability, presumably due to membrane damage during injection (Figure 3b,d and Figure S9a, Supporting Information).[5b] In contrast, the presence of 25×10^{-3} M **2** significantly increased the cell viability to 87% after injection, which is similar to the viability of cells encapsulated in identically prepared hydrogels without injection (Figure 3b,d and Figure S9a, Supporting Information). Our strategy is equally effective to protect mesenchymal stem cells (MSCs), significantly improving their viability during injection when the catalyst was incorporated in the hydrogels (Figure S11, Supporting Information). These results strongly indicated that the enhanced network dynamics of hydrogels in the presence of the catalyst improved injectability and offered better protection for encapsulated cells during flow.

Long-term stability of hydrogel scaffolds is often required to provide support for cell adhesion and growth after cell injection. Rapid hydrogel erosion is a common challenge for many dynamic and injectable hydrogels. We hypothesized that rapid passive diffusion of the dissolved small molecule catalyst away from the hydrogel post-injection would slow down the dynamic exchange of hydrazone cross-links and thus enhance the hydrogel stability. We therefore monitored the diffusion of **2**, which was incorporated in the hydrogel at either 25 or 50×10^{-3} M initial concentration, into the buffer solution after injection by monitoring its absorption at 281 nm. After 50 µL hydrogel was injected and immersed in 1 mL PBS, 60% of **2** diffused out of the hydrogel within 1 h, and only less than 1%

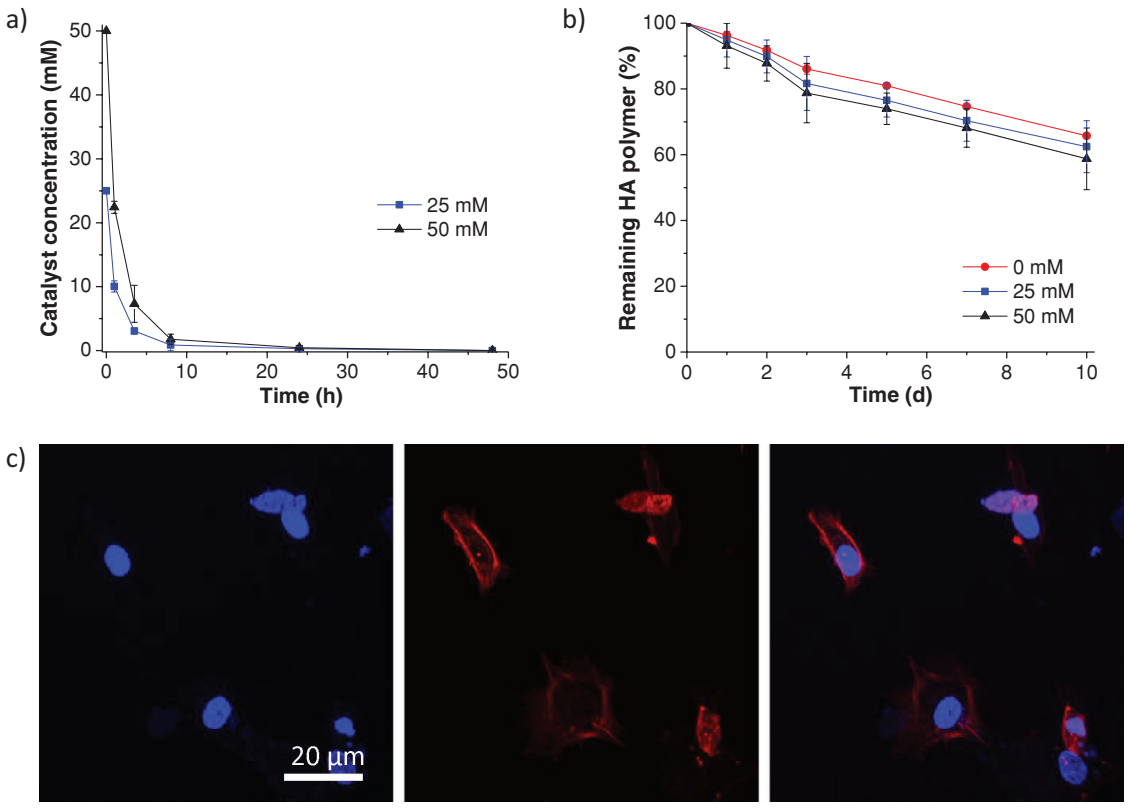

Figure 4. a) Concentration of remaining catalyst **2** inside hydrogels over time after immersion of catalyst-containing hydrogels in PBS, showing rapid diffusion out of the hydrogel. b) Erosion kinetics of hydrogels with and without catalyst **2** at 37 °C over 10 d. c) Cell spreading in hydrogels 72 h post-injection with initially 25×10^{-3} M **2** during injection (Left panel: blue DAPI nuclear staining; middle panel: red actin cytoskeleton staining; right panel: merged image).

remained inside the gel after 8 h (**Figure 4**a). Due to the rapid diffusion of catalyst, hydrogels after catalyst removal exhibited almost identical properties as those without an incorporated catalyst (Figure S12, Supporting Information). To examine whether the rapid diffusion and thus removal of catalyst could increase the long-term stability of the hydrogels, we compared the erosion rate of hydrogels with different initial concentrations of incorporated catalyst. Hydrogels without incorporated catalyst exhibited an initial erosion rate of 3.5% d^{-1} (over 10 d), as determined by fitting the erosion data to a zero-order kinetic model, and 65% of the hydrogel mass was retained after 10 d. Hydrogels initially containing 25 or 50×10^{-3} M catalyst **2** had erosion rates of 3.8 and 4.1% d^{-1}, respectively, similar to those without a catalyst (Figure 4b), presumably due to rapid diffusion of **2** out of the hydrogels. In contrast, when diffusion of **2** away from the hydrogel was prevented by immersing the hydrogel into a buffer solution containing 25×10^{-3} M **2**, the hydrogel was completely dissolved within 12 h (Figure S14, Supporting Information). Therefore, our strategy temporally modulates the exchange rate of dynamic cross-linking, achieving the desired short-term injectability and long-term stability at different stages of the application from the same hydrogel network.

To test the ability of our HA hydrogels to support cellular growth as a scaffold after injection, we attached cell-adhesive RGD peptide motifs to the hydrazine-functionalized HA polymer. HUVECs were encapsulated within the RGD-presenting HA-hydrazone hydrogels in the presence of 25×10^{-3} M **2**, injected through a 28 G needle into a Petri dish, and cultured under physiological conditions in EBM-2 medium for 3 d. Cell morphology was analyzed by staining and imaging of the cell nuclei and actin cytoskeleton. HUVECs encapsulated within the hydrogels demonstrated high viability and a spread morphology (Figure 4c, Figure S15, Supporting Information). In contrast, significant cell death was observed when cultured in HA gels without RGD peptides for 3 d (Figure S16, Supporting Information).

In summary, we have developed a new strategy to temporally modulate the exchange kinetics of dynamically cross-linked hydrogels using a biocompatible organocatalyst to enable high injectability and high stability as required at different stages of cell delivery. In this strategy, the cytocompatible sulfonated amino-benzimidazole functions as an effective catalyst to temporally accelerate the rates of formation and exchange of dynamic covalent hydrazone cross-links in HA-based hydrogels. As a result, the presence of a catalyst enhances the rates of gelation and stress relaxation, but neither alters the hydrogel network structure nor its storage modulus, which allowed us to *independently* and *continuously* tune the stiffness and stress-relaxation rate of the hydrogels by varying the polymer concentration and catalyst loading, respectively. The accelerated exchange of cross-linking led to enhanced injectability of the hydrogels and improved cell protection during injection. As the catalyst rapidly diffused out of the hydrogels after injection, the hydrogels gained high stability and slow erosion

post-injection to provide a long-term, cell-adhesive scaffold for cell culture. This simple yet effective design bestows hydrogels with both high injectability and stability, two often conflicting but desired properties of dynamic hydrogels used for biomedical applications. Moreover, this strategy is not limited to HA-based hydrogels, but can be easily applied to any other polymer scaffolds or mixed matrices with desirable durability or degradability. Considering the broad applications of biocompatible hydrazone chemistry, we envision this strategy to be applicable to a wide range of dynamic hydrogel materials for therapeutic cell delivery and 3D printing of encapsulated cell scaffolds.

Supporting Information

Supporting information is available from the Wiley Online Library or from the author.

Acknowledgements

The authors gratefully acknowledge seed funding from the Bio-X Program at Stanford University. The authors thank Prof. E.T. Kool, Dr. L. Cai, Dr. C.M. Madl, and Dr. H. Wang for helpful discussions. S.C.H. acknowledges funding support from the National Science Foundation (DMR 1508006).

Conflict of Interest

The authors declare no conflict of interest.

Keywords

dynamic covalent chemistry, hydrogels, organocatalysis, polymer networks

Received: September 11, 2017
Revised: February 17, 2018
Published online:

[1] a) B. Jeong, Y. H. Bae, D. S. Lee, S. W. Kim, *Nature* **1997**, *388*, 860; b) H. J. Chung, T. G. Park, *Nano Today* **2009**, *4*, 429; c) J. A. Yang, J. Yeom, B. W. Hwang, A. S. Hoffman, S. K. Hahn, *Prog. Polym. Sci.* **2014**, *39*, 1973.

[2] M. Guvendiren, H. D. Lu, J. A. Burdick, *Soft Matter* **2012**, *8*, 260.

[3] a) E. A. Appel, J. del Barrio, X. J. Loh, O. A. Scherman, *Chem. Soc. Rev.* **2012**, *41*, 6195; b) H. Y. Wang, S. C. Heilshorn, *Adv. Mater.* **2015**, *27*, 3717; c) A. M. Rosales, K. S. Anseth, *Nat. Rev. Mater.* **2016**, *1*, 15012; d) L. J. Dooling, M. E. Buck, W. B. Zhang, D. A. Tirrell, *Adv. Mater.* **2016**, *28*, 4651; e) V. Yesilyurt, M. J. Webber, E. A. Appel, C. Godwin, R. Langer, D. G. Anderson, *Adv. Mater.* **2016**, *28*, 86; f) Y. L. Zhang, L. Tao, S. X. Li, Y. Wei, *Biomacromolecules* **2011**, *12*, 2894; g) M. M. Pakulska, K. Vulic, R. Y. Tam, M. S. Shoichet, *Adv. Mater.* **2015**, *27*, 5002.

[4] a) L. Haines-Butterick, K. Rajagopal, M. Branco, D. Salick, R. Rughani, M. Pilarz, M. S. Lamm, D. J. Pochan, J. P. Schneider, *Proc. Natl. Acad. Sci. USA* **2007**, *104*, 7791; b) H. D. Lu, M. B. Charati, I. L. Kim, J. A. Burdick, *Biomaterials* **2012**, *33*, 2145; c) T. C. Tseng, L. Tao, F. Y. Hsieh, Y. Wei, I. M. Chiu, S. H. Hsu, *Adv. Mater.* **2015**, *27*, 3518; d) H. Y. Wang, D. Q. Zhu, A. Paul, L. Cai, A. Enejder, F. Yang, S. C. Heilshorn, *Adv. Funct. Mater.* **2017**, *27*, 1605609; e) L. Li, B. Yan, J. Q. Yang, L. Y. Chen, H. B. Zeng, *Adv. Mater.* **2015**, *27*, 1294.

[5] a) B. D. Olsen, J. A. Kornfield, D. A. Tirrell, *Macromolecules* **2010**, *43*, 9094; b) B. A. Aguado, W. Mulyasasmita, J. Su, K. J. Lampe, S. C. Heilshorn, *Tissue Eng., Part A* **2012**, *18*, 806.

[6] a) C. Q. Yan, A. Altunbas, T. Yucel, R. P. Nagarkar, J. P. Schneider, D. J. Pochan, *Soft Matter* **2010**, *6*, 5143; b) C. Q. Yan, M. E. Mackay, K. Czymmek, R. P. Nagarkar, J. P. Schneider, D. J. Pochan, *Langmuir* **2012**, *28*, 6076.

[7] a) H. D. Lu, D. E. Soranno, C. B. Rodell, I. L. Kim, J. A. Burdick, *Adv. Healthcare Mater.* **2013**, *2*, 1028; b) L. Y. Shi, F. L. Wang, W. Zhu, Z. P. Xu, S. Fuchs, J. Hilborn, L. J. Zhu, Q. Ma, Y. J. Wang, X. S. Weng, D. A. Ossipov, *Adv. Funct. Mater.* **2017**, *27*, 1700591; c) K. Y. Zhang, Q. Feng, J. B. Xu, X. Y. Xu, F. Tian, K. W. K. Yeung, L. M. Bian, *Adv. Funct. Mater.* **2017**, *27*, 1701642; d) L. Cai, R. E. Dewi, S. C. Heilshorn, *Adv. Funct. Mater.* **2015**, *25*, 1344; e) M. J. Glassman, J. Chan, B. D. Olsen, *Adv. Funct. Mater.* **2013**, *23*, 1182; f) C. B. Rodell, N. N. Dusaj, C. B. Highley, J. A. Burdick, *Adv. Mater.* **2016**, *28*, 8419; g) C. B. Rodell, J. W. MacArthur, S. M. Dorsey, R. J. Wade, L. L. Wang, Y. J. Woo, J. A. Burdick, *Adv. Funct. Mater.* **2015**, *25*, 636.

[8] a) A. Dirksen, S. Dirksen, T. M. Hackeng, P. E. Dawson, *J. Am. Chem. Soc.* **2006**, *128*, 15602; b) A. Dirksen, S. Yegneswaran, P. E. Dawson, *Angew. Chem., Int. Ed.* **2010**, *49*, 2023; c) E. T. Kool, D. H. Park, P. Crisalli, *J. Am. Chem. Soc.* **2013**, *135*, 17663.

[9] a) D. D. McKinnon, D. W. Domaille, J. N. Cha, K. S. Anseth, *Adv. Mater.* **2014**, *26*, 865; b) B. P. Purcell, D. Lobb, M. B. Charati, S. M. Dorsey, R. J. Wade, K. N. Zellars, H. Doviak, S. Pettaway, C. B. Logdon, J. A. Shuman, P. D. Freels, J. H. Gorman, R. C. Gorman, F. G. Spinale, J. A. Burdick, *Nat. Mater.* **2014**, *13*, 653; c) O. P. Oommen, S. J. Wang, M. Kisiel, M. Sloff, J. Hilborn, O. P. Varghese, *Adv. Funct. Mater.* **2013**, *23*, 1273; d) M. Patenaude, T. Hoare, *Biomacromolecules* **2012**, *13*, 369; e) Z. Wei, J. H. Yang, Z. Q. Liu, F. Xu, J. X. Zhou, M. Zrinyi, Y. Osada, Y. M. Chen, *Adv. Funct. Mater.* **2015**, *25*, 1352; f) X. F. Yang, G. Q. Liu, L. Peng, J. H. Guo, L. Tao, J. Y. Yuan, C. Y. Chang, Y. Wei, L. N. Zhang, *Adv. Funct. Mater.* **2017**, *27*, 1703174.

[10] a) P. Crisalli, E. T. Kool, *Org. Lett.* **2013**, *15*, 1646; b) D. Larsen, M. Pittelkow, S. Karmakar, E. T. Kool, *Org. Lett.* **2015**, *17*, 274.

[11] a) J. A. Burdick, G. D. Prestwich, *Adv. Mater.* **2011**, *23*, H41; b) X. Xu, A. K. Jha, D. A. Harrington, M. C. Farach-Carson, X. Q. Jia, *Soft Matter* **2012**, *8*, 3280.

[12] J. Lou, R. S. Stowers, S. Nam, Y. Xia, O. Chaudhuri, *Biomaterials* **2018**, *154*, 213.

[13] a) T. J. Lampidis, C. Castello, A. Delgiglio, B. C. Pressman, P. Viallet, K. W. Trevorrow, G. K. Valet, H. Tapiero, N. Savaraj, *Biochem. Pharmacol.* **1989**, *38*, 4267; b) S. Y. Jiang, Z. Q. Cao, *Adv. Mater.* **2010**, *22*, 920.